Magnetic-field and temperature dependence of the energy gap in InN nanobelt

K. Aravind, Y. W. Su, D. S. Chung, Watson Kuo, C. S. Wu, K. S. Chang-Liao, K. H. Chen, L. C. Chen, and C. D. Chen

Citation: AIP Advances **2**, 012155 (2012); doi: 10.1063/1.3691830

View online: http://dx.doi.org/10.1063/1.3691830

View Table of Contents: http://scitation.aip.org/content/aip/journal/adva/2/1?ver=pdfcov

Published by the AIP Publishing

Magnetic-field and temperature dependence of the energy gap in InN nanobelt

K. Aravind,[1,2,a] Y. W. Su,[2,a] D. S. Chung,[2] Watson Kuo,[3] C. S. Wu,[4] K. S. Chang-Liao,[1] K. H. Chen,[5] L. C. Chen,[6] and C. D. Chen[2,7,b]
[1]*Department of Engineering and System Science, National Tsing Hua University, Hsinchu 300, Taiwan*
[2]*Institute of Physics, Academia Sinica, Nankang 115, Taipei, Taiwan*
[3]*Department of Physics, National Chung Hsing University, Taichung 402, Taiwan*
[4]*Department of Physics, National Chang-Hua University of Education, ChangHua 500, Taiwan*
[5]*Institute of Atomic and Molecular Sciences, Academia Sinica, Taipei 106, Taiwan*
[6]*Center for Condensed Matter Sciences, National Taiwan University, Taipei 106, Taiwan*
[7]*Department of Physics, National Cheng Kung University, Tainan 701, Taiwan*

(Received 6 December 2011; accepted 6 February 2012; published online 23 February 2012)

We present tunneling measurements on an InN nanobelt which shows signatures of superconductivity. Superconducting transition takes place at temperature of 1.3K and the critical magnetic field is measured to be about 5.5kGs. The energy gap extrapolated to absolute temperature is about 110μeV. As the magnetic field is decreased to cross the critical magnetic field, the device shows a huge zero-bias magnetoresistance ratio of about 400%. This is attributed to the suppression of quasiparticle subgap tunneling in the presence of superconductivity. The measured magnetic-field and temperature dependence of the superconducting gap agree well with the reported dependences for conventional metallic superconductors. [http://dx.doi.org/10.1063/1.3691830]

Among the III-nitride semiconductors, InN has attracted much attention because of the discovery of its narrow direct band gap around 0.7 eV [Ref. 1 and 2]. It was found that the Fermi level at InN surfaces is pinned well above the conduction band edge, leading to strong surface band bending and electron accumulation. The accumulation of conduction electrons at the surface states increases the carrier concentration and, thus, provides a better conductivity than other semiconductors [Ref. 3]. The first observation of superconductivity in highly disordered two-dimensional InN film at 3K by Inushima *et al.* [Ref. 4] raises a fundamental controversial issue concerning the coexistence of semiconductor and superconductivity. Subsequent studies by the same group revealed the dependence of superconducting transition temperature on the carrier concentration [Ref. 5]. They concluded that neither the surface electron accumulation layer nor the In-metal precipitation is the main cause of the superconductivity. Rather, the superconductivity is attributed to Josephson coupling between In-layers which are intercalated by nitrogen layers [Ref. 6]. The inter-chain superconducting coupling in the *ab*-plane was further supported by Ling *et al.* [Ref. 7] who studied InN films of wurtzite structure. The objective of our present work is to explore possible superconductivity in InN nanobelts. Nanostructures with typical rectangular cross section are often termed as nanobelts [Ref. 8]. To this end, transport measurement on devices comprising of a single nanobelt was carried out, and both temperature and magnetic field dependence of the superconducting gap was investigated. The results are in agreement with a model of a nano-superconducting object connected to electrodes via tunnel junctions.

---

[a]These authors contributed equally to this work
[b]Corresponding author email: chiidong@phys.sinica.edu.tw

Single crystalline InN nanobelts were synthesized from indium powder with Au catalyst grown by a guided-stream thermal chemical vapor deposition technique under a NH_3 gas flowing. The growth method was previously reported in detail by Hu *et al.* [Ref. 8]. The nanobelts have typical width ranging from 20 to 200 nm, a width to thickness ratio of 2-10 and lengths of up to several tens of micrometers. The InN nanobelts were subsequently extracted into suspension in isopropanol solvent by short ultrasonic agitation. A few droplets of the dispersion were spread over Si substrate with μm-sized measurement pads pre-fabricated on 300-nm-thick SiO_2 surface. After drying, the wires strongly adhered to the substrate due to van der Waals interaction; this adhesion allows us to perform the subsequent device fabrication procedures. Optical microscopy and scanning electron microscopy (SEM) were then employed to select and locate the individual nanobelts. For device fabrication, polymethylmethacrylate (PMMA) resist was first spun onto the substrate and nano-scaled patterns for contact electrodes were then exposed by an electron beam writer. The exposed resist was developed, creating a template for contact electrodes, this is followed by a oxygen reactive ion etching (RIE) cleaning process in order to remove resist contamination on the contact area. After that, Au/Ni metal wires with 50/50nm in thickness served as electrodes were deposited by thermal evaporation at a pressure of 7×10^{-7} torr. Finally, the resist was dissolved in acetone, lifting off the unwanted metal film on the top of the resist and leaving the contact electrodes. Shown in the lower inset of Fig.1(a) is an SEM image of the measured InN nanobelt device. The width of this particular nanobelt is about 65 nm, and the separation between the source and drain electrodes is approximately 200 nm.

For electrical characterization a symmetric circuit with a low-noise current-voltage amplifier was employed, and the devices were symmetrically biased with respective to the ground. Low temperature measurements were performed using a He^3/He^4 dilution refrigerator. The IV_b characteristic was linear at room temperature with a resistance of about 30 kΩ. As the temperature was lowered to 0.35K the asymptotic resistance increased by two times and the device displayed a suppression of current at low V_b region, as shown in Fig. 1(a), leading to a dip in the differential conductance, $G_d=dI/dV_b$. One of the possible explanations for the conductance dip is Coulomb blockade of electron tunneling due to appreciable charging energy associated with the smallness of the nanobelt. One of the criterions for the appearance of Coulomb blockade is, the contact resistance R_C between the leads and the nanobelt should be greater than the quantum resistance $R_K\equiv h/e^2 \approx 26\text{k}\Omega$ [Ref. 9]. The asymptotic resistance of this device at low temperature is about 65kΩ, and our previous study [Ref. 10] suggested that the nanobelt resistance is small compared to the contact resistance, therefore the assumption that $R_C>R_K$ is justified.

Magnetic field dependence of the IV_b characteristic was studied. The applied magnetic field was perpendicular to the chip plane. As the magnetic field increases, the conductance dip is getting shallow and the width of the dip becomes narrower. In magnetic fields greater than 5.5kGs, denoted as B_c, the width as well as the depth of the conductance dip becomes field independent. Shown in Fig. 1(b) is an intensity plot of the differential conductance as a function of both bias voltage V_b and magnetic field B. The conductance dip corresponds to the darker area of the intensity plot. We noticed that for $|B| > B_c$ the dotted curves stay a constant in bias voltage which we denote as V_1. For $|B| < B_c$, the dotted curves, denoted as V_2, increases with decreasing B. We note that V_2 comprises of two parts: a constant part which equals to V_1 and an additional B dependent part. Assuming the device contains two identical tunnel junctions between the nanobelt and the source/drain electrodes, the constant value V_1, about $2E_C/e$=0.17 mV, is attributed to Coulomb blockade due to the charging effect which is insensitive to the magnetic field. Here E_C is the charging energy. Now, V_2 contains a magnetic field dependent component, which we denote as $2\Delta(B)$. Where $2\Delta(B)$ is a gap edge energy and is identified as the peak position of the 2nd derivative of IV_b curves. The peak positions are plotted in Fig. 1(c) and the extracted $\Delta(B)$ can be very well described by the predicted field dependence of superconducting energy gap by the theory:[11]

$$\Delta(B)/\Delta(0) = [1 - (\frac{B}{B_c})^2]^{1/2} \quad (1)$$

We believe that this is a strong evidence of the presence of superconductivity in this InN nanobelt. Δ(B=0) denotes the zero-field energy gap and is found to be about 95 μeV at T=0.35K.

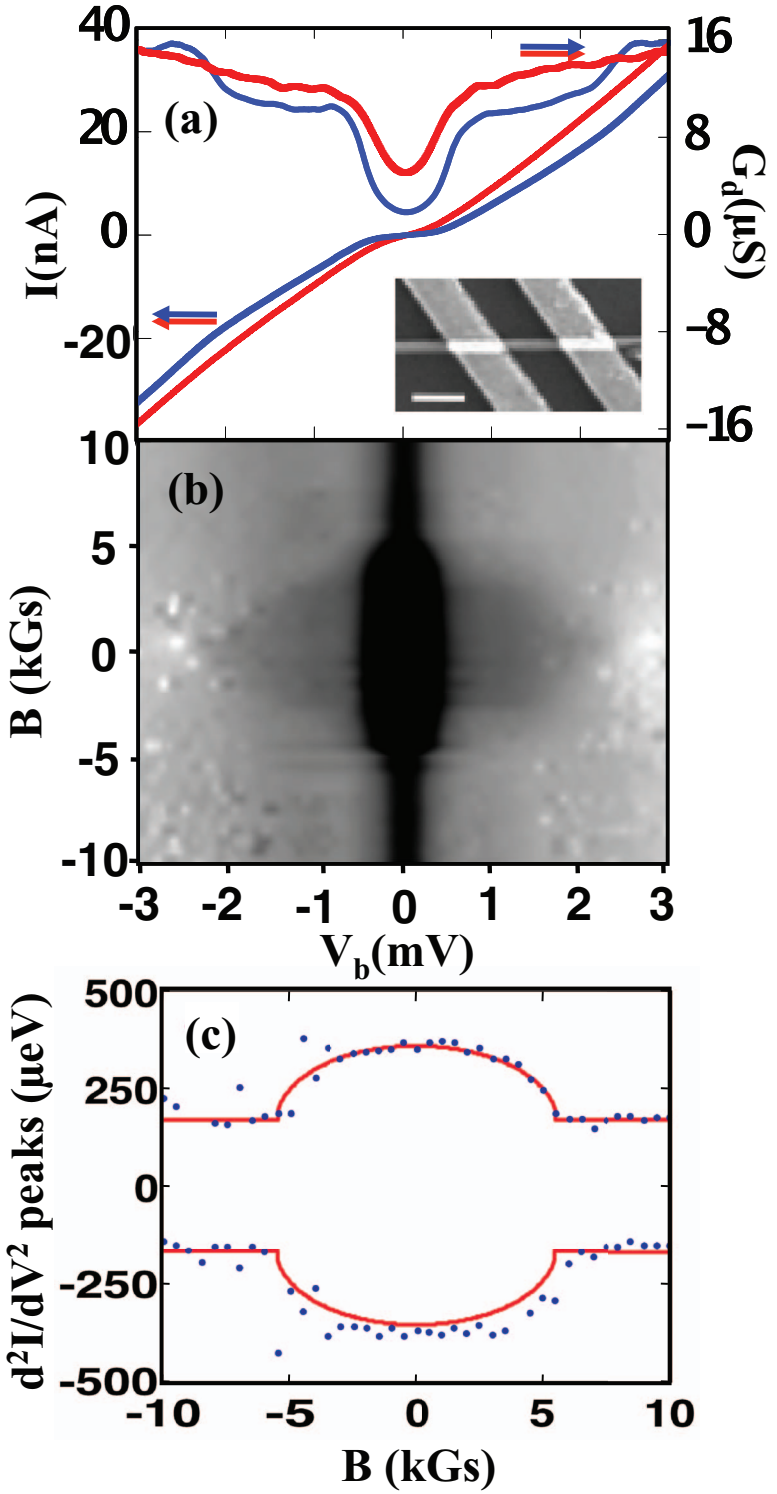

FIG. 1. (color online) (a) Traces of current (center curves) and differential conductance (upper curves) versus bias voltage at B=0 (blue) and 5.5kGs (red). At zero-field and low bias voltage, a prominent conductance dip opens up. The SEM image in the lower inset shows the measured device. The scale bar is 200nm. (b) Intensity plot of differential conductance G_d as a function of B and V_b. At $V_b < V_1$, G_d is independent of magnetic field. The data were taken at T≈350mK. (c) The energy gap (blue dots) extracted from IV_b in varying B is plotted along with the BCS prediction (red curve) given in Eq. (1).

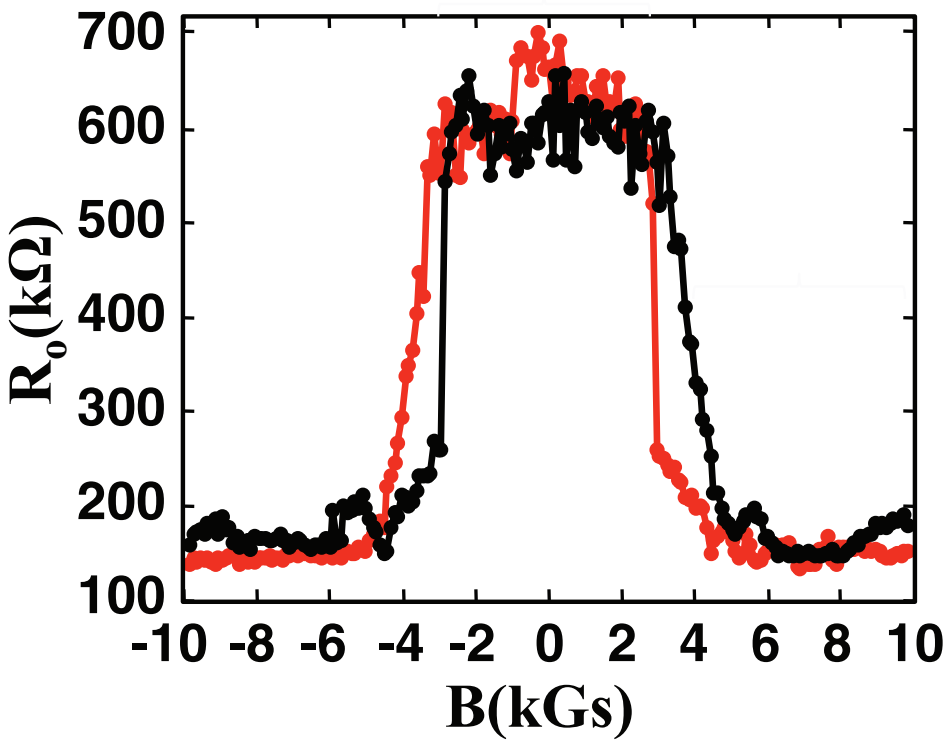

FIG. 2. (color online) Electric measurement of zero-resistance (R_0) as a function of magnetic field for InN devices. The black and red traces correspond to the positive and negative sweep directions, respectively. The magnetic field is directed perpendicular to the substrate at 0.35K.

Further, at low bias voltages, we probed the quasiparticle subgap resistance at zero-bias as the magnetic field was swept across the critical magnetic field B_c. The curves shown in Fig. 2 are zero-bias resistance (R_0) extracted from IV_b characteristics for perpendicular magnetic field ramped back and forth between -10kGs and +10kGs at $T \approx 0.35$K. The small hysteresis structure at a field of about ±1kGs is a manifestation of the coercivity field of the Ni-electrode. Notice that a magnetoresistance plateau with sharp edges appears in fields ranging between -5.5kGs and +5.5kGs. The plateau with an average R_0 value of about 650 kΩ corresponds to a huge magnetoresistance ratio of about 400%. The magnetoresistance drops to a value of 150kΩ as the magnetic field $|B|$ was brought to beyond 5.5kGs. This is reconfirmation of the critical field value obtained in Fig. 1. In high fields, the magnetoresistance does not change with magnetic field and remains at 150kΩ because applied filed is greater than B_c. The high resistance (650kΩ) at the plateau is an indication that the nanobelt is in the superconducting state and we are measuring the quasiparticle subgap resistance of the superconducting belt. At fields greater than B_c, the superconductivity is quenched and the zero-bias resistance is decreased dramatically due to diminishing superconducting gap. The zero-bias resistance is, however, remaining at a value (150kΩ) much higher than the asymptotic resistance (65kΩ) due to the Coulomb blockade.

Next, temperature dependence of the superconducting gap in the same InN nanobelt was studied and is shown in Fig.3. As temperature increases, the Coulomb blockade becomes less significant. At 4K, the IV_b curve becomes linear and the conductance dip vanishes, indicating that the charging energy is smaller than 4K. The temperature dependence of the superconducting gap is measured and is shown in Fig. 3(b). Our measured data suggests a T_c of about 1.3K and $\Delta(0)$ of 110μeV when extrapolated to absolute temperature. This corresponds to a $2\Delta(0)/k_BT_C$ value close to 2, which is lower than the predicted BCS ratio of 3.4 [Ref. 11]. The small BCS ratio could be a consequence of the interface with the proven surface charge states on the InN nanobelt [Ref. 12] or it could be arising from the exotic double gap superconductivity along the reports in some compound

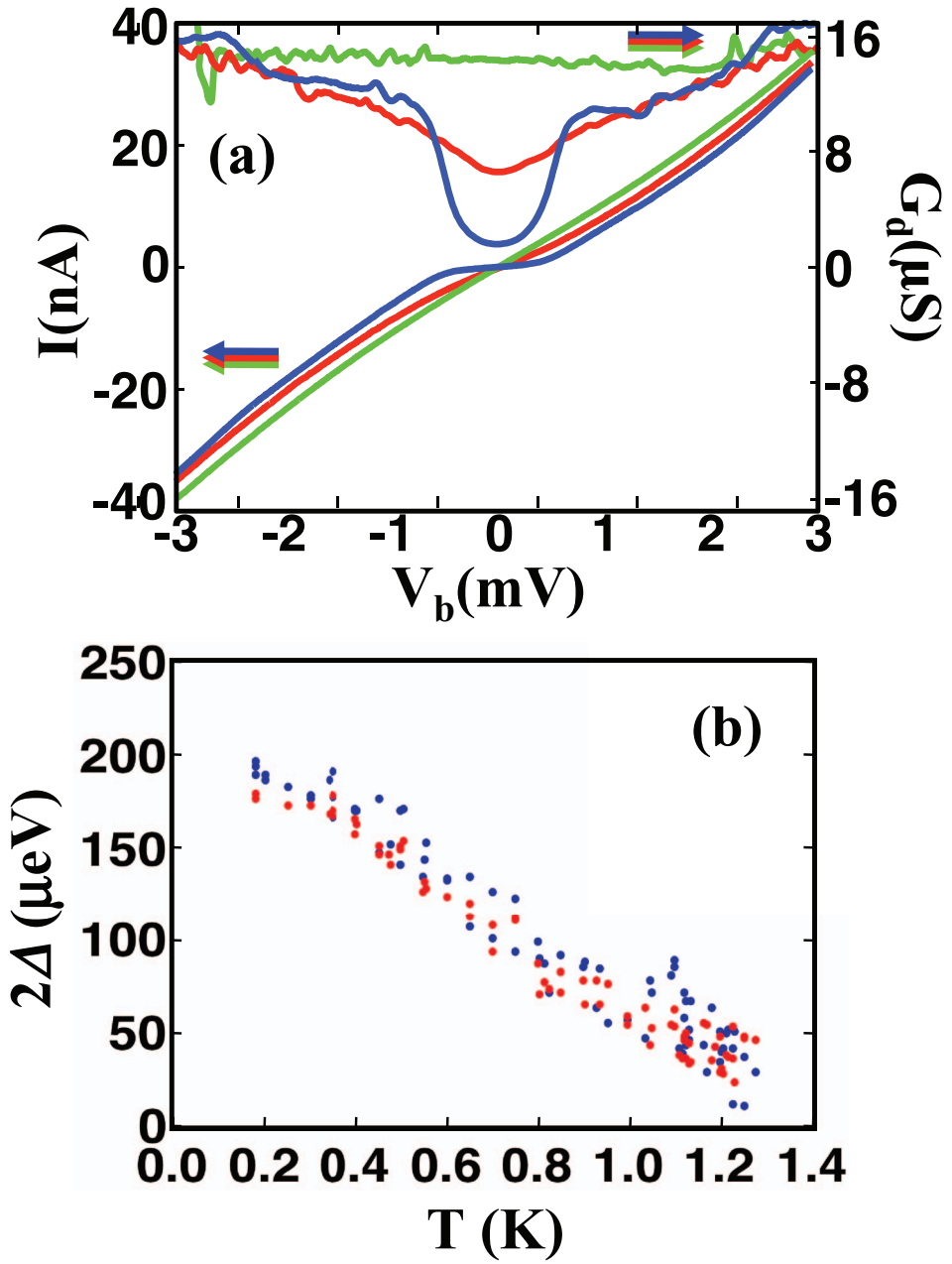

FIG. 3. (color online) (a) Current (center curves) and conductance (upper curves) versus bias voltage characteristics at three temperatures: 0.18K (blue), 0.85K (red), and 4K (green). (b) The extracted energy gap as a function of temperature. Red and blue dots represent data extracted from positive and negative sides of the IV_b characteristics.

superconductors [Ref. 13]. The latter is supported by the conductance structure at $V_b \approx 2.5$mV (e.g. the blue conductance curve in Fig. 1(a)), which implying a large superconducting gap Δ_L. The conductance intensity plot shown in Fig. 1(b) suggests that this Δ_L is suppressed almost linearly by the applied magnetic field, but unfortunately this feature is too smeared for an elaborated study on the temperature dependence. At this stage, this low BCS ratio remains an open question; intense experimental and theoretical understanding is not available till date on this subject and there could be very interesting physics to uncover.

Inushima *et al.* [Refs. 4–6 and references cited in Ref. 6] and Ling *et al.* [Ref. 7] have observed superconductivity in InN films and reported superconducting transition between 0.12K and 3.5K,

depending on the carrier concentration. They also observed supercurrent in these films. However, the device we studied does not display supercurrent feature. Instead, the zero-bias resistance increased at low temperatures. The reason for the absence of supercurrent in our device is the following: it is well known that in a superconductor, phase and charge are quantum conjugate variables. Localization of charges (Cooper pairs) due to Coulomb blockade causes quantum fluctuations of the superconducting phase [Ref. 14]. When phase fluctuates strongly, global superconductivity is destroyed and supercurrent is diminished. Further, localization of charges gives rise to an increased zero-bias resistance at low temperatures and that explains the enhanced Coulomb blockade characteristics seen in Fig. 1(a). The E_J/E_c ratio for this device is approximately 5.5μeV/85μeV and the device is in $E_J << E_c$ regime which reconfirms the absence of supercurrent, where E_J is the Josephson energy and E_c is the charging energy. Technically, even if there were any small supercurrent present, it would be hard to observe due to the two-probe measurement configuration involving two large resistors in series with nanobelt.

In summary, we present here the precursors of superconductivity in an InN nanobelt. The superconducting gap and the transition temperature are found to be 110μeV and 1.3K, respectively. The superconducting gap can be suppressed by an applied magnetic field perpendicular to the belt, and the critical field is about 5500Gs. The suppression as a function of the field strength follows a dependence similar to that reported for superconducting films. Further, the superconducting gap decreases at elevated temperatures, following the theoretical prediction for superconducting films. Magnetic field dependence of the zero-bias resistance displays a plateau in magnetic fields smaller than the critical magnetic field, corresponding to a huge magnetoresistance ratio. The experiment reveals signatures of superconductivity in the InN nanobelt.

[1] J. Wu, W. Walukiewicz, K. M. Yu, J. W. Ager III, E. E. Haller, H. Lu, W. J. Schaff, Y. Saito, and Y. Nanishi, Appl. Phys. Lett. **80**, 3967 (2002).
[2] Q. X. Guo, M. Nishio, H. Ogawa, A. Wakahara and A. Yoshida, Phys. Rev. B **58**, 15304 (1998); T. L. Tansley and C. P. Foley, J. Appl. Phys. **59**, 3241 (1986).
[3] I. Mahboob, T. D. Veal, C. F. McConville, H. Lu and W. J. Schaff, Physical Review Letters **92**, 036804 (2004); I. Mahboob, T. D. Veal, L. F. J. Piper, C. F. McConville, Hai Lu, W. J. Schaff, J. Furthmüller and F. Bechstedt, Phys. Rev. B **69**, 201307 (2004).
[4] T. Inushima, V. V. Mamutin, V. A. Vekshin, S. V. Ivanov, T. Sakon, S. Motokawa, and S. Ohoya, J. Cryst. Growth **227**, 481 (2001).
[5] T. Inushima, Science and Technology of Advanced Materials **7**, S112 (2006); T. Inushima, M. Higashiwaki, T. Matsui, T. Takenobu, and M. Motokawa, Phys. Rev. B **72**, 085210 (2005).
[6] T. Inushima, N. Kato, T. Takenobu and M. Motokawa, Phys. Stat. Sol. (a) **203**, 80 (2006).
[7] D. C. Ling, J. H. Cheng, Y. Y. Lo, C. H. Du, A. P. Chiu, C. A. Chang, and P. H. Chang, Phys. Stat. Sol. (b) **244**, 4594 (2007).
[8] M. S. Hu, W. M. Wang, T. T. Chen, L. S. Hong, C. W. Chen, C. C. Chen, Y. F. Chen, K. H. Chen, and L. C. Chen, Adv. Funct. Mater. **16**, 537 (2006).
[9] H. S. J. van der Zant, W. J. Elion, L. J. Geerligs, and J. E. Mooij, Phys.Rev B **54**, 10081 (1996).
[10] Y. W. Su, K. Aravind, C. S. Wu, Watson Kuo, K. H. Chen, L. C. Chen and K. S. Chang-Liao, W. F. Su and C. D. Chen, J. Phys. D: Appl. Phys. **42**, 185009 (2009).
[11] M. Tinkham, *Introduction to superconductivity*, 2nd edition, 18-19 and page 63, Dover publications, Inc (1996).
[12] K. Aravind, Y. W. Su, I. L. Ho, C. S. Wu, K. S. Chang-Liao, W. F. Su, K. H. Chen, L. C. Chen, and C. D. Chen, App.Phys.Lett **95**, 092110 (2009) and references therein.
[13] F. Giubileo, D. Roditchev, W. Sacks, R. Lamy, D. X. Thanh, and J. Klein, Phys. Rev. Lett. **87**, 177008 (2001); F. Giubileo, D. Roditchev, W. Sacks, R. Lamy and J. Klein, Europhys. Lett. **58**, 764 (2002).
[14] D. B. Haviland and Per Delsing, Phys. Rev. B **54**, R6857 (1996).